Supporting Information for

Ionic environment affects bacterial lipopolysaccharide packing and function

Ali Rahnamoun[†], *Kyoungtea Kim*[‡], *Joel A. Pedersen*[‡,§], *and Rigoberto Hernandez*[*†]

[†] Department of Chemistry, Johns Hopkins University, Baltimore, Maryland 21218, United States
[‡] Molecular and Environmental Toxicology Center, University of Wisconsin-Madison, Madison, Wisconsin 53706, United States
[§] Departments of Soil Science, Chemistry, Civil & Environmental Engineering, University of Wisconsin-Madison, Madison, Wisconsin 53706, United States

This document includes the following supporting information:

- Table S1 provides several parameters for the model systems.
- Table S2 providing the parameters used in running all experiments reported in the Main document using inductively coupled plasma-mass spectrometry (ICP-MS).
- Table S3 reports the mean molecular areas $\hat{A}_m$ obtained experimentally at several different values, as indicated, of the compression modulus, K_A. The largest of these values (50 $mN \cdot m^{-1}$) corresponds to the transition from the LE to the liquid condensed (LC) state. An intermediate compression indicated here (20 $mN \cdot m^{-1}$) is approximately the monolayer pressure equivalent to a tensionless bilayer and exceeds that at the G-to-LE transition (10 $mN \cdot m^{-1}$). The intermediate value (20 $mN \cdot m^{-1}$) is also used for comparison between experiment and simulation in the Main document. The latter were performed under "tensionless" fluid lipid bilayers conditions which have been seen[1] to correspond to those in the LE state of lipid monolayers at the air–water interface.
- Table S4 compares the mean molecular areas from this work to those in prior work.[2-7]
- Figure S1 provides a representative decay of $\hat{A}_m$ observed in a simulation as a function of the integration time of the trajectory.
- Figure S2 illustrates how the model system was broken up into stages for the calculation of the potential between OAH and the bilayer using ABF.
- Figure S3 provides a comparison of the original and augmented radii in the CHARMM force field
- Figure S4 shows representative snapshots of configurations of the Ca^{2+} bridge in an arbitrarily selected trajectory.
- Figure S5 displays a representative snapshot of the location of OAH with respect to the LPS bilayer at which minimum free energy is observed.

Table S1. Number of phosphoryls, Kdo sugars and charge of the deep rough LPS of *Salmonella enterica.*[a]

Phosphoryl groups Per LPS	Kdo Units Per LPS	Charge Per LPS	Total Phosphoryl groups	Total Kdo units	Total Charge
2	3	–7	100	150	-350

[a] Each LPS bilayer contains 50 LPS molecules in the simulation box.

Table S2. Inductively coupled plasma-mass spectrometry (ICP-MS) instrument and acquisition parameters.

ICP-MS operating conditions	**Calibration and sensitivity**
RF Generator [W]	Calibration: 4-2000 µg/L
Forward power: 1260	^{69}Ga @ 10 µg/L for internal standard
Reflected power: < 2	Medium Resolution Isotopes reported: ^{24}Mg, ^{44}Ca
Argon gas flows [L·min^{-1}]	Sample uptake: 0.4 mL/min
Nebulizer: 0.92	Sensitivity ^{24}Mg = 17166 cps/ppb
Auxiliary: 0.88	Sensitivity ^{44}Ca = 1011 cps/ppb
Coolant: 16.0	Matrix spike: (100 µg/L)
	CRM: SLRS-6
Data acquisition conditions	
Dwell time: 0.010 s	
20 sample points/peak	
Sweeps/reading: 4	
Number of readings: 4	
Mass window: 125 %	
Peak integration window: 60 %	
Dual counting/analog detector mode	

Table S3. Mean molecular areas of interfacial LPS monolayers in the presence of alkali and alkaline earth cations obtained experimentally at the indicated compression moduli.[a]

Added Cation	**K_A (mN/m) =**	**$\hat{A}_m$ (Å^2)**			***n***
		10	**20**	**50**	
none		233 ± 2.6	230 ± 3.3	211 ± 4.0	3
Na^+		191 ± 1.1	190 ± 1.0	174 ± 3.3	4
K^+		198 ± 2.4	195 ± 2.5	180 ± 3.3	4
Ca^{2+}		191 ± 3.7	190 ± 3.4	183 ± 2.3	4
Mg^{2+}		197 ± 3.5	198 ± 1.3	185 ± 2.4	4

[a] Abbreviations: $\hat{A}_m$, mean molecular area; K_A, compression modulus; *n* = number of replicates.

Table S4. Selected experimental mean molecular areas for monolayers of lipopolysaccharides from surface pressure–area isotherms [a]

LPS type	strain [b]	cation(s)	[cation] (mM)	other solution constituents	Π (mN·m^{-1})	$\hat{A}_m$ (Å^2)	T (K)	ref.
Re	S1	–	–	–	20	182 ± 2.3 [c]	294	this work
		–	–	–	35	157 ± 1.7 [c]	294	this work
		Na^+	3	–	20	147 ± 1.1 [c]	294	this work
		Na^+	3	–	35	132 ± 1.4 [c]	294	this work
		K^+	3	–	20	152 ± 1.8 [c]	294	this work
		K^+	3	–	35	132 ± 2.1 [c]	294	this work
		Ca^{2+}	1.5	–	20	154 ± 2.2 [c]	294	this work
		Ca^{2+}	1.5	–	35	134 ± 1.3 [c]	294	this work
		Mg^{2+}	1.5	–	20	157 ± 2.8 [c]	294	this work
		Mg^{2+}	1.5	–	35	139 ± 2.3 [c]	294	this work
		Na^+	100	5 mM HEPES, pH 7.4	20	~168	293	2
		Na^+	100	5 mM HEPES, pH 7.4	35	~134	293	2
		Na^+/Ca^{2+}	100/50	5 mM HEPES, pH 7.4	20	~138	293	2
		Na^+/Ca^{2+}	100/50	5 mM HEPES, pH 7.4	35	~126	293	2
		Na^+	100	5 mM HEPES, pH 7.4	20	~168	293	3
		Na^+/Ca^{2+}	100/50	5 mM HEPES, pH 7.4	20	~170	293	3
		–	–	10 mM phosphate buffer, pH 7.2	30	~120 [d,e]	283	4
		Na^+	100	10 mM phosphate buffer, pH 7.2	30	~120 [d,e]	283	4
		Ca^{2+}	50	–	30	~120 [d,e]	283	4
		Na^+/Ca^{2+}	100/50	–	30	~120 [d,e]	283	4
Rc	E1	Na^+	20?	20 mM sodium phosphate, pH 7.0	20	~107	RT [f]	5
		Na^+	20?	20 mM sodium phosphate, pH 7.0	35	~92	RT [f]	5
Ra	S2	Na^+	100	5 mM HEPES, pH 7.4	20	~205	293	2
		Na^+	100	5 mM HEPES, pH 7.4	35	~180	293	2
		Na^+/Ca^{2+}	100/50	5 mM HEPES, pH 7.4	20	~164	293	2
		Na^+/Ca^{2+}	100/50	5 mM HEPES, pH 7.4	35	~138	293	2
	E2	Na^+	150	10 mM HEPES, pH 7.4	35	188 ± 1.3	294	6
		Na^+/Ca^{2+}	150/50	1 mM EDTA, 10 mM HEPES, pH 7.4	35	156 ± 3.2	294	6
wild type	E3	Na^+	100	10 mM HEPES, pH 7.4	15	~300 [e]	RT [f]	7
		Na^+/Ca^{2+}	100/20	10 mM HEPES, pH 7.4	15	~250 [e]	RT [f]	7

[a] Abbreviations: $\hat{A}_m$, mean molecular area; RT, room temperature; T, temperature; Π, monolayer lateral pressure. [b] Bacterial strains: E1, *Escherichia coli* J5; E2, *E. coli* K-12; E3, *E. coli* O55:B5; S1, *Salmonella enterica* serovar minnesota R595; S2, *S. enterica* serovar minnesota R60. [c] Purified salts. [d] LPS in native salt form. [e] Salts used as received. [f] Assumed.

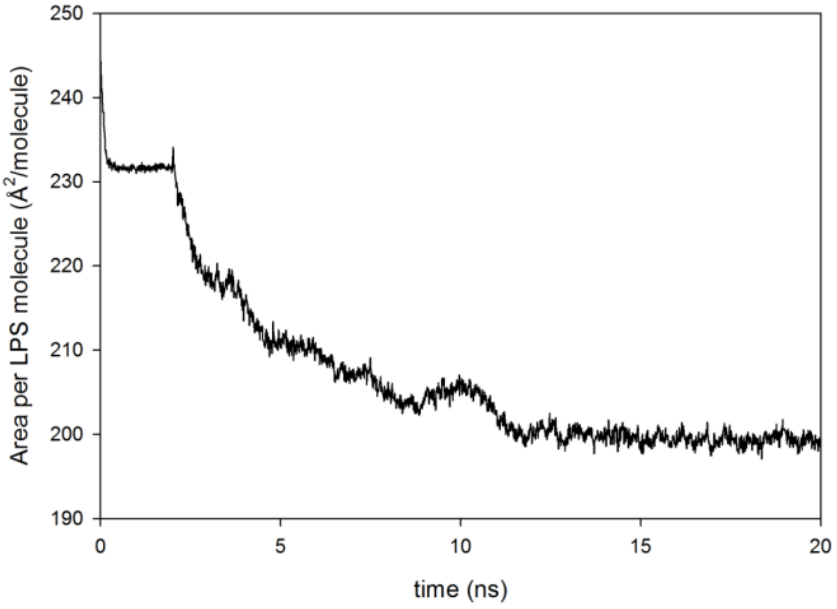

Figure S1. Evolution of the effective mean molecular area ($\hat{A}_{m)}$ molecule during a single trajectory equilibration of deep rough *Salmonella enterica* in Ca^{2+} ionic environment.

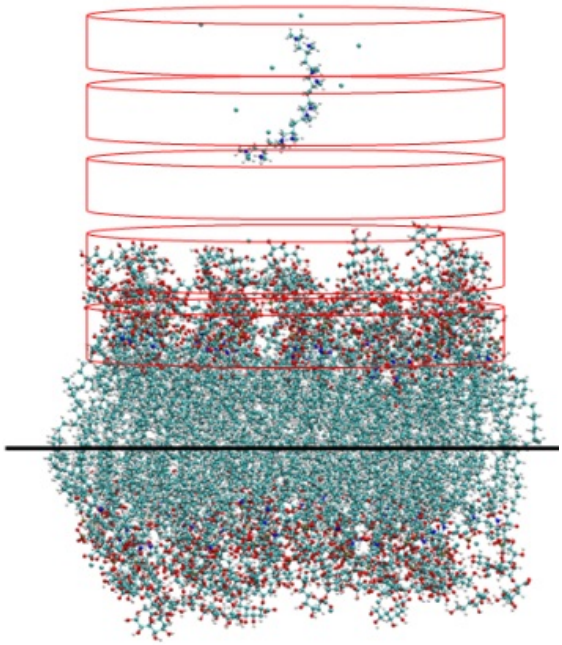

Figure S2. ABF sampling while the COM distance between OAH and the carbon atoms of the acyl chain terminal methyl group of the lipid A sections of the LPS molecules is changing from 50 Å to 10 Å. The sampling areas in separate ABF calculations are shown with red cylindrical shapes.Implicit water solvent molecules are not shown for clarity.

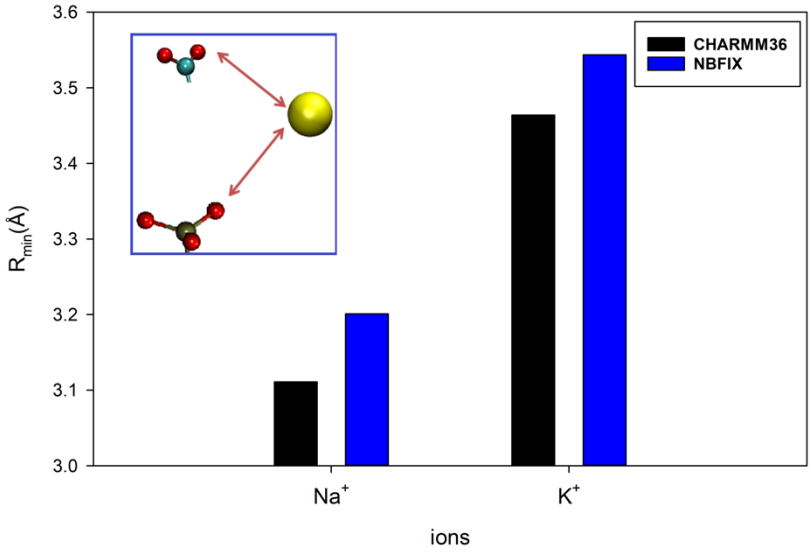

Figure S3. Original and augmented CHARMM LJ radii for the interactions between monovalent cations and oxygen atoms of carboxyl and phosphoryl groups. Pair-specific non-bonded interactions between monovalent cations and oxygen atoms of carboxyl and phosphoryl groups. LJ radii of these pair interactions were calibrated against experimentally measured quantities.

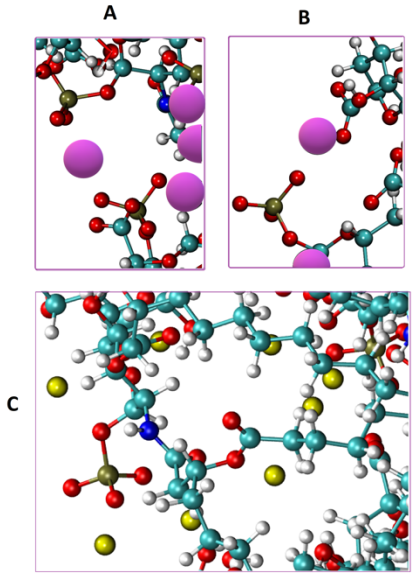

Figure S4. Sample snapshots of a Ca^{2+} bridge between (A) phosphoryl–phosphoryl and (B) carboxyl–phosphoryl groups in the core region of deep rough LPS from *Salmonella enterica*. Carbon atoms are shown in cyan, Oxygen atoms are shown in red, Hydrogen atoms are shown in white and Phosphorous atoms are shown in dark gold. The Ca^{2+} ions are shown in purple. (C) Sample snapshot of charge shielding of anionic groups by K^+ monovalent cation. Na^+ ions are shown in yellow.

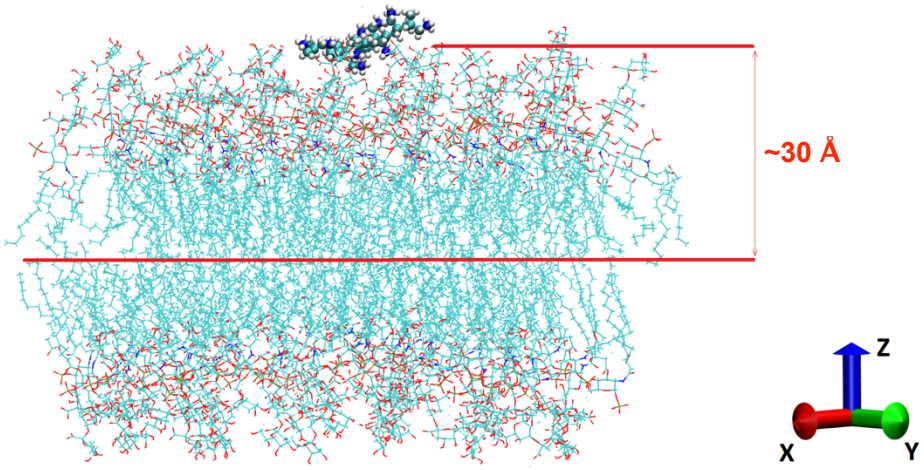

Figure S5. Snapshot of the location of OAH with respect to the LPS bilayer at which minimum free energy is observed.

References

1. Marsh, D. Lateral pressure in membranes. *Biophys. Biochim. Acta* **1996,** *1286*, 183-223.
2. Herrmann, M.; Schneck, E.; Gutsmann, T.; Brandenburg, K.; Tanaka, M. Bacterial lipopolysaccharides form physically cross-linked, two-dimensional gels in the presence of divalent cations. *Soft Matter* **2015,** *11*, 6037-6044.
3. Oliveira, R. G.; Schneck, E.; Quinn, B. E.; Konovalov, O. V.; Brandenburg, K.; Gutsmann, T.; Gill, T.; Hanna, C. B.; Pink, D. A.; Tanaka, M. Crucial roles of charged saccharide moieties in survival of gram negative bacteria against protamine revealed by combination of grazing incidence x-ray structural characterizations and Monte Carlo simulations. *Phys. Rev. E* **2010,** *81*.
4. Jeworrek, C.; Evers, F.; Howe, J.; Brandenburg, K.; Tolan, M.; Winter, R. Effects of specific versus nonspecific ionic interactions on the structure and lateral organization of lipopolysaccharides. *Biophys. J.* **2011**, 2169-77.
5. Le Brun, A. P.; Clifton, L. A.; Halbert, C. E.; Lin, B.; Meron, M.; Holden, P. J.; Lakey, J. H.; Holt, S. A. Structural characterization of a model Gram-negative bacterial surface using lipopolysaccharides from rough strains of *Escherichia coli*. *Biomacromolecules* **2013,** *14*, 2014-2022.
6. Hwang, H.; Paracini, N.; Parks, J. M.; Lakey, J. H.; Gumbart, J. C. Distribution of mechanical stress in the *Escherichia coli* cell envelope. *Biochim. Biophys. Acta* **2018,** *1860*, 2566-2575.
7. Micciulla, S.; Gerelli, Y.; Schneck, E. Structure and conformation of wild-type bacterial lipopolysaccharide layers at air-water interfaces. *Biophys. J* **2019,** *116*, 1259-1269.